Marine and Petroleum Geology 57 (2014) 537–545

Contents lists available at ScienceDirect

Marine and Petroleum Geology

journal homepage: www.elsevier.com/locate/marpetgeo

Research paper

Comparison of evolutionary and static modeling of stresses around a salt diapir

Maria A. Nikolinakou [a, *], Michael R. Hudec [a], Peter B. Flemings [b]

[a] Bureau of Economic Geology, The University of Texas at Austin, 10100 Burnet Road, Building PRC-130, Austin, TX 78758, USA
[b] Jackson School of Geosciences, The University of Texas at Austin, 10100 Burnet Road, Building PRC-130, Austin, TX 78758, USA

ARTICLE INFO

Article history:
Received 1 April 2014
Received in revised form
11 June 2014
Accepted 3 July 2014
Available online 11 July 2014

Keywords:
Static modeling
Forward modeling
ABAQUS
ELFEN
Salt diapir
Poro-elastoplasticity
Wellbore stability
Drained analysis

ABSTRACT

We compare an evolutionary with a static approach for modeling stress and deformation around a salt diapir; we show that the two approaches predict different stress histories and very different strains within adjacent wall rocks. Near the base of a rising salt diapir, significantly higher shear stresses develop when the evolutionary analysis is used. In addition, the static approach is not able to capture the decrease in the hoop stress caused by the circumferential diapir expansion, nor the increase in the horizontal stress caused by the rise of the diapir. Hence, only the evolutionary approach is able to predict a sudden decrease in the fracture gradient and identify areas of borehole instability near salt. Furthermore, the evolutionary model predicts strains an order of magnitude higher than the strains within the static model. More importantly, the evolutionary model shows significant shearing in the horizontal plane as a result of radial shortening accompanied by an almost-equivalent hoop extension. The evolutionary analysis is performed with ELFEN, and the static analysis with ABAQUS. We model the sediments using a poro-elastoplastic model. Overall, our results highlight the ability of forward evolutionary modeling to capture the stress history of mudrocks close to salt diapirs, which is essential for estimating the present strength and anisotropic characteristics of these sediments.

1. Introduction

During the last two decades, understanding the stress, material behavior, and pore pressure around salt bodies has become increasingly important. Many wells have encountered drilling problems near salt, leading to additional expense or even abandonment (Dusseault et al., 2004; Meyer et al., 2005; Willson et al., 2003; Zhang et al., 2008). In addition, new plays have been discovered beneath allochthonous and autochthonous salt, making it necessary to drill through the salt body to reach the target (Adachi et al., 2012; Beltrão et al., 2009; Mackay et al., 2008).

Salt and the evolution of its cross section to the present day geometry has been studied extensively using kinematic restorations (Rowan and Ratliff, 2012). Such studies aim to explain the observed geologic cross section through a sequence of plausible past sections; however, they do not look into stresses within the sediments. Similarly, large-strain numerical studies (Albertz and Beaumont, 2010; Albertz et al., 2010; Allen and Beaumont, 2012; Chemia et al., 2009; Goteti et al., 2012; Gradmann et al., 2009; Schultz-Ela, 2003) have focused on the geologic evolution of salt systems without modeling the geomechanical response of the wall rocks. On the other hand, geomechanical analyses can provide estimates of the stress field and pore pressure around salt; such analyses are necessary in order to design the most economic well path, ensure borehole stability, and minimize the risk of wellbore fracturing and formation fluid influxes.

Most geomechanical studies around salt have used the *static* approach, in which the model is built using the present-day salt geometry and an assumed initial stress field. Most published studies assume idealized salt geometries (Fredrich et al., 2003; Luo et al., 2012a; Nikolinakou et al., 2012; Orlic and Wassing, 2013; Sanz and Dasari, 2010), but a few studies use geometries devised on the basis of seismic information (Henk, 2005; Koupriantchik et al., 2005, 2004; Nikolinakou et al., 2013). The initial stress field usually assumes uniaxial strain deposition (a given horizontal-to-vertical stress ratio), meaning that shear stresses are present within the salt body at the beginning of the analysis. The static analyses are driven by the fact that the salt, being viscous, cannot

* Corresponding author. Tel.: +1 512 471 0415.
E-mail addresses: mariakat@mail.utexas.edu, mariakat@alum.mit.edu (M.A. Nikolinakou), michael.hudec@beg.utexas.edu (M.R. Hudec), pflemings@jsg.utexas.edu (P.B. Flemings).

http://dx.doi.org/10.1016/j.marpetgeo.2014.07.002
0264-8172/

sustain deviatoric stresses, and so it deforms to achieve an isostatic stress state (Schutjens et al., 2010; Urai and Spiers, 2007). Deformation of the salt body places stress loads on neighboring sediments and, as discussed in the studies referenced above, causes stress perturbations, stress rotations, and pore pressure changes. The static analyses are able to capture a significant part of the salt–sediment interaction, and for this reason the energy industry has developed elaborate three-dimensional static geomechanical tools. However, static analyses cannot account for stress or pore-pressure changes that develop as a result of the evolution of the salt geometry to its current shape.

Geomechanical *evolutionary* models, on the other hand, can simulate the development of the salt cross section to its final geometry. Contrary to certain static models (and to restoration studies), this final salt geometry does not match the real present-day geometry observed in seismic sections. However, evolutionary models provide a powerful tool to simulate and understand how stresses re-distribute in the wall rocks near a moving salt.

The major benefits of the evolutionary models are the following:

a) Evolutionary models simulate sedimentation concurrently with the evolution of the salt section. The stresses within the basin develop as a function of both the depositional process and the loading from the salt. The models do not assume that the horizontal stresses develop as a ratio of the vertical during sedimentation (i.e., uniaxial strain deposition (Matthews and Kelly, 1967; Zoback and Healy, 1984)).
b) Evolutionary models simulate the accumulation of strain (resulting from mechanical and/or non-mechanical processes), and hence maintain a memory of the loading history. Such a memory is essential for determining the current strength and deformation characteristics of mudrocks (Terzaghi et al., 1996).

In comparison to static analyses, evolutionary ones require longer preparation and run times and greater computational power. Furthermore, the industry has already invested in static modeling tools. Therefore, investigation and quantification of the improvement in stress predictions achieved by the evolutionary analyses is important. In this article we compare the poro-elastoplastic stress changes around a salt diapir, as predicted by a static analysis performed using ABAQUS (Version 6.9), with the stress changes predicted by an evolutionary analysis performed using ELFEN (Rockfield, 2010). Sanz et al. (2011) made a similar comparison, using the same finite-element tools, but did not include deformations and loading histories. We extend their work and show that the evolutionary approach predicts much higher strains and dissimilar stress histories, with final shear stresses that are different at vital parts of the model.

2. Finite-element models

We compare a static model run within the finite-element program ABAQUS (Version 6.9) with an evolutionary model developed within the finite-element program ELFEN® (Rockfield, 2010). Because of its versatility, robustness, and open interface allowing user-developed material models, ABAQUS™ has been employed extensively within the energy industry for the development of static models. Combining the implicit porous response with the large deformations associated with deposition and salt movement is more challenging. We employ ELFEN® for the evolutionary analyses because it offers a forward modeling technology that is based on a finite strain, quasi-static, explicit, Lagrangian formulation, complemented by automated adaptive remeshing techniques. In addition, ELFEN® can simulate sedimentation and includes computational features developed for the modeling of salt diapirs (Peric and Crook, 2004; Thornton et al., 2011).

2.1. Model set-up

For the evolutionary model that we construct in ELFEN, we use an axisymmetric model to describe a three-dimensional salt diapir (rotation of the cross section shown in Fig. 1, Nikolinakou et al. (2014)). Because the structure is axisymmetric, all horizontal sections are circular. Initially, the salt is 12 km thick at the center of the diapir and 6 km thick beneath the far-field sedimentary basin. The initial sedimentary basin is 6.25 km thick at the far-field boundary ($r = 20$ km, Fig. 1). The top of the salt diapir is buried by 250 m of sediment. There is no slip between the diapir and the basin. The base and side boundaries are rollers (zero-normal-displacement, free-slip boundaries), and the model is wide enough that the side boundary is unaffected by any stress perturbations. The initial stresses in the model are geostatic, with a horizontal-to-vertical effective stress ratio of $K_0 = 0.8$ for the sediments and $K_0 = 1$ for the salt. Pore pressures are assumed to be hydrostatic and do not change during the analysis (drained simulation). We simulate sedimentation by aggrading the top of the model to horizontal horizons in increments of 400 m every 500,000 years. The local thickness of the aggraded layer is determined by the surface topography prior to sedimentation. The volume of salt remains constant throughout the simulation.

We model the salt as a solid viscoplastic material using a reduced form of the Munson and Dawson formulation (1979). This is a constitutive model that provides a unified approach to both creep and plasticity and is formulated such that the salt viscosity is a function of both effective stress and temperature. The density is constant and equal to 2200 kgr/m^3, and the equivalent salt viscosity ranges from 10^{18} to 10^{20} Pa s. Basin sediments are modeled as porous elastoplastic, using the SR3 constitutive model from the Elfen® material library (Rockfield, 2010). This model is based on the principles of Critical State soil mechanics (same family as Modified Cam Clay (Muir Wood, 1990)), but it is characterized by a modified yield surface (Crook et al., 2006). For the purpose of this study, we chose the input parameters such that the calibrated SR3 yield surface is very similar to the Modified Cam Clay one. The density is a function of porosity (Fig. 1), and porosity is constantly updated as a function of the stress changes caused by sedimentation and salt loading. Further discussion about the materials used and the

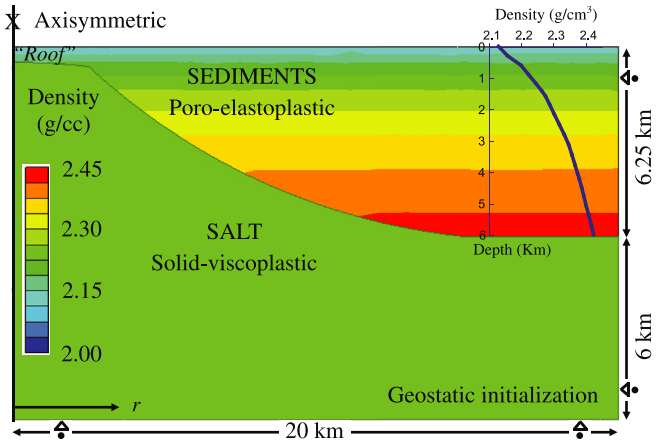

Figure 1. Initial vertical section of evolutionary numerical model prior to sedimentation. Initial diapir = 12 km high at center and basin = 6.25 km deep at edge of model. Contours and inner plot show initial density–depth profile (after Nikolinakou et al., 2014).

structure of the numerical mesh can be found in Nikolinakou et al. (2014); detailed material input for the evolutionary model can be found in Appendix A (Tables A1 and A2).

In our comparative analysis, we assume that sediment aggrades for a total of 2 million years, followed by a one-million year period of quiescence (no sedimentation) that allows the stresses within the model to equilibrate (Fig. 2) (Nikolinakou et al., 2014).

The geometry of the evolutionary model after 2 million years of sedimentation is imported as the present-day, initial geometry for the static analysis (Fig. 3, built using ABAQUS™). For the static analysis, we model the salt as viscoelastic, with a constant density of 2200 kgr/m^3 and an equivalent salt viscosity of 10^{18} Pa s. We model the sediments as poro-elastoplastic, with the Modified Cam Clay model and a constant density of 2230 kgr/m^3, representing the average density in the evolutionary model. Detailed material input for the static model can be found in Appendix A (Tables A3 and A4). As in the evolutionary model, there is no slip between the diapir and the basin, and the base and side boundaries are rollers (free-slip boundaries). For the stress initialization, we use a horizontal-to-vertical effective stress ratio of 0.8 for the basin and the equivalent horizontal-to-vertical stress ratio of 0.87 for the salt, imposed to ensure initial horizontal equilibrium (assuming hydrostatic pore pressures) (Nikolinakou et al., 2012).

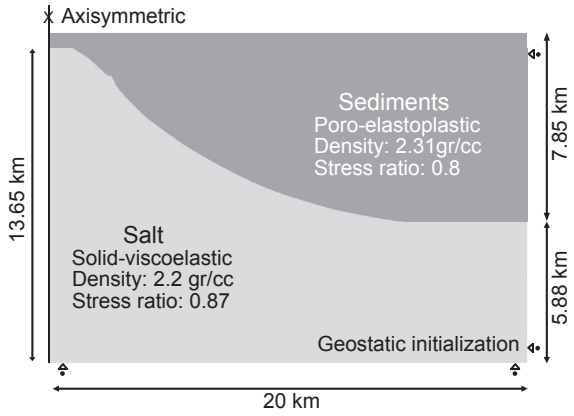

Figure 3. Initial geometry used for static model (vertical section), based on geometry of evolutionary model after 2 m.y. of sedimentation (Fig. 2b).

2.2. Loading mechanism

The mechanism that drives the analysis is different in the two simulations; consequently, the interaction between the salt and the sediments is also different. In the evolutionary model, stresses increase with time because of the sedimentation process. At the same time, this sedimentation creates a density imbalance between the basin and the salt; this results in stresses within the salt that are higher than the integration of overburden (i.e., the salt is overpressurized relative to its density gradient). As a result, the salt moves upwards and expands outwards (Fig. 4a). The growth of the diapir radius compresses the wall rocks, thereby increasing the radial (horizontal) stress. At the same time, the diapir expansion in the hoop (circumferential) direction subjects the wall rocks to extension that substantially decreases the hoop stress (Nikolinakou et al., 2014). Thus the final stresses within the wall rocks develop as a function of sediment weight as well as salt loading (Fig. 2). Note that, because the salt is flowing, shear stresses within the diapir remain minimal throughout the analysis.

In the static model, on the other hand, the stress relaxation within the salt is the main mechanism that loads the wall rocks. As part of the geostatic stress initialization, we assign horizontal-to-vertical stress ratios to both the sediments and the salt. This results in deviatoric stresses within the salt, which eventually deforms to relax to an isostatic stress state (Fredrich et al., 2003). The mode of deformation during static stress relaxation can vary depending on the form of the salt. The stresses within salt bodies with comparable horizontal and vertical dimensions (ideally, spheres) converge to an isostatic value that lies between the overburden value and that of the initial horizontal stresses (Fredrich et al., 2003; Luo et al., 2012a; Nikolinakou et al., 2012; Sanz and Dasari, 2010); In a typical extensional setting, this causes loading at the flank and unloading above and/or below the salt. On the other hand, stresses within long, shallow salt bodies converge to the value of the overburden, because no arching mechanism can develop to support any stresses not transmitted through the salt (Nikolinakou et al., 2013). This loads the sediments laterally. In our model, the diapir is connected to a large salt base (ours is an axisymmetric model, so the base is a cylinder with a radius of 20 km and an average height of 6 km). This base is loaded by the weight of the sediments; hence, the stresses within the salt are dictated by the maximum basin overburden found away from the diapir ($r > 15$ km). This results in a salt stress that is higher than the sediment horizontal stresses. Therefore, the salt deforms outwards in the radial direction and expands in the hoop (circumferential) direction (Fig. 4b), causing an increase in the horizontal stress (compressive loading) and a decrease in the hoop stress (extensional loading) within the neighboring wall rocks. The modes of deformation appear similar to those in the evolutionary simulation (Fig. 4). However, the loading mechanism in the static analysis is driven by the relaxation of shear stresses, while the loading mechanism in the evolutionary analysis is the result of an ongoing sedimentation coupled with the rise of the diapir.

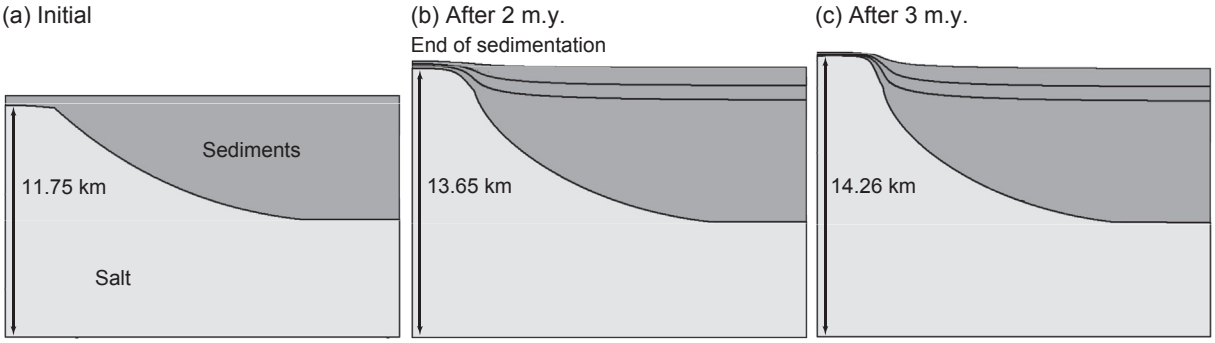

Figure 2. Vertical sections showing geometry changes of evolutionary model: (a) initial configuration (Fig. 1); (b) end of sedimentation, after 2 m.y.; (c) after additional 1-m.y. period of quiescence. The deposited layers are also shown.

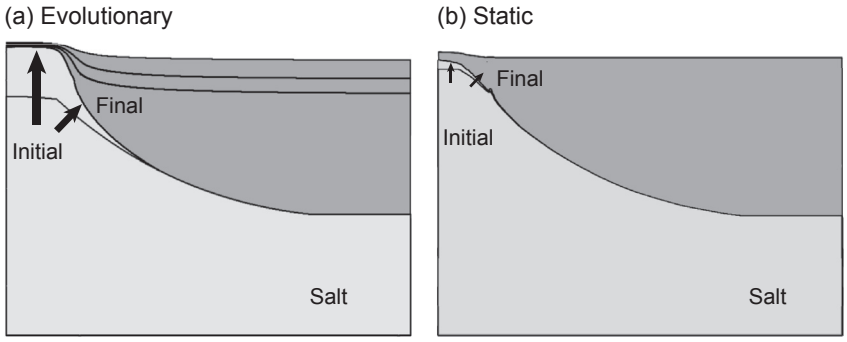

Figure 4. Initial and final salt geometries for (a) evolutionary and (b) static model. Final geometry for the evolutionary model obtained after 2 m.y. of aggradation, and additional 1 m.y. of quiescence. Arrows illustrate movement of salt.

3. Comparison of stresses between evolutionary and static analyses

In our analyses, the pattern of stress changes in the static model is similar to that of the evolutionary model, but the magnitude is much smaller (Fig. 5). The static model cannot capture the large deformations and, consequently, cannot generate the large stress changes associated with the rising and expanding diapir in the evolutionary model (Fig. 4). The larger increase in horizontal stress and larger decrease in hoop stress within the evolutionary model relative to the static model yields higher shear stresses, especially near the base of the diapir (Fig. 5).

A stress–path plot (Fig. 6) demonstrates the evolution of stresses during the simulation. The stress path describes the way that effective mean stress (σ') and shear stress (q) evolve during the analysis, and hence represents changes in both the volumetric response (associated with the effective mean stress) and shearing. The two modes of analysis predict different stress paths for a sediment element located close to the base of the diapir, within the area of maximum shear stress (Point A, highlighted on Fig. 5). The path for the evolutionary model is shown in a solid line, starting from the open circle and ending on the filled circle (Fig. 6); the path for the static is shown in a dashed line, from the open square to the filled square.

Both elements are initialized on the uniaxial compression line (dashed arrow line on Fig. 6). This line represents stress states that result from uniaxial loading (no lateral strains) and therefore they are characterized by a constant ratio of vertical to horizontal effective stress ($K_0 = 0.8$). The evolutionary model is initialized at a lower level of mean and shear stress (open circle, Fig. 6) than that exhibited in the static model (open square, Fig. 6). This difference arises because the initial (present-day) stage for the static model corresponds to a time 2 m.y. into the sedimentation history of the evolutionary model, during which 1600 m of sediments have been deposited (Fig. 2).

Both stress paths have a similar trend: they show only minor change in the mean stress and an increase in the shear stress. The low amount of change in the mean stress is a result of the significant hoop-stress decrease near the diapir that counterbalances the stress increase because of the ongoing deposition (Nikolinakou et al., 2014). On the other hand, this decrease in the hoop stress leads to an increase of shear stresses, especially in the horizontal plane (the difference between the radial and the hoop stress increases). The two stress paths are similar, but the evolutionary analysis predicts significantly higher shear levels than does the static analysis in this part of the model (Point A), because the evolutionary one is able to simulate the larger circumferential expansion associated with the diapir rise—a process not captured by the static analysis (Fig. 4). The evolutionary analysis predicts a stress path that approaches the critical state line (Fig. 6; in this non-triaxial stress setting, the critical state line is approximated for the last stress point, as described by Lewis and Schrefler (1987), Rockfield (2010)). This proximity of the stress path to the critical state indicates that the sediments near the base of a salt diapir may actually be much closer to shear failure than would be predicted by static analysis.

The higher shear predicted by simulating the evolution of the salt-body volume has major implications for borehole stability (Fig. 7). To avoid failure or collapse of the borehole during drilling, the mud weight must be higher than the formation pore pressure in order to avoid blowouts; mud weight must also be lower than the least principal stress in order to avoid fracturing and loss of circulation. In addition, the range of admissible borehole pressures is limited by the possibility of compressive failure of the borehole: the

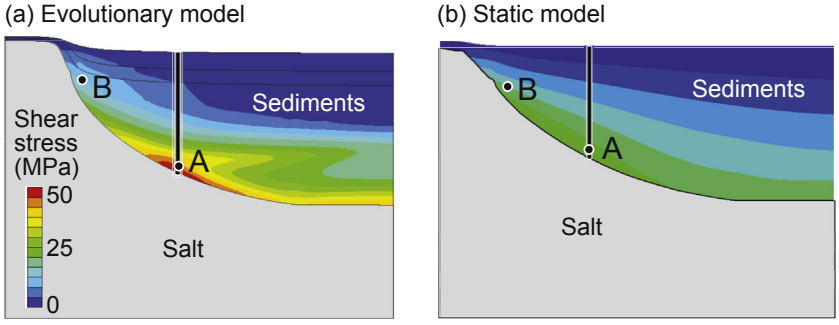

Figure 5. Shear stresses: (a) Evolutionary model: end stage of simulation, after 2 m.y. of aggradation, and additional 1 m.y. of no sedimentation; and (b) Static model, end stage of simulation, after all shear stresses within salt have relaxed.

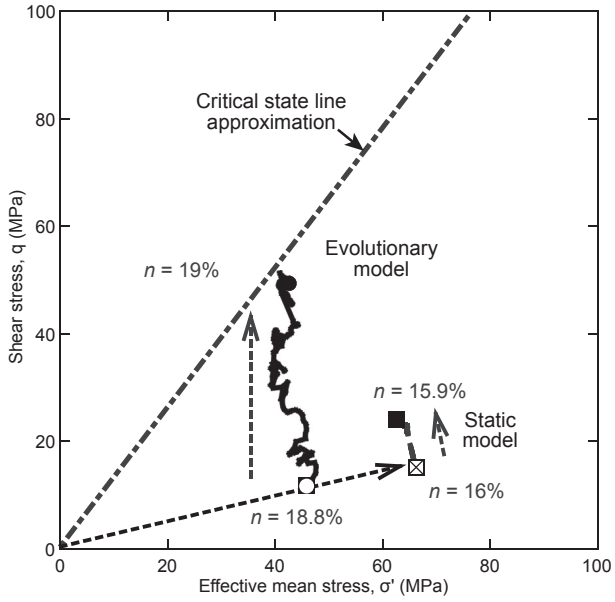

Figure 6. Plot of mean effective stress and corresponding shear stress (stress path) during evolutionary and static analyses for Point A, near base of diapir (Fig. 5). Open and solid circles mark initial and final stages, respectively, for evolutionary model; blank and solid squares show initial and final stages for static model. Evolutionary approach predicts much higher shear stresses and stress state closer to critical state line.

width of the zone of shear failure (breakouts) should be less than 180° (Luo et al., 2012b; Zoback, 2007). We calculate the range of admissible mudweights for a vertical well profile through A (Fig. 5), based on the evolutionary results (Fig. 7a) and the static results (Fig. 7b). Near the base of the diapir (the area of maximum shear), the evolutionary model predicts a sudden decrease in the least principal stress, which – if not anticipated – can cause loss of circulation. More importantly, the shear increase is so substantial that no possible mud weight could exert enough pressure to prevent borehole breakouts (Fig. 7a). In contrast, the static model shows no notable changes in the least principal stress nor in the desired mud weight range with depth (Fig. 7b).

Whereas Point A is located in the zone of most pronounced stress difference between the two approaches (Fig. 5), Point B, near the upper part of the diapir, represents an area where the final stress states are similar. Despite this similarity in the final state, the stress histories are very different (Fig. 8). The evolutionary approach predicts an increase in the mean effective stress, owing mainly to significant increase in the horizontal stress because of the expanding diapir. This increase in mean stress causes a decrease in porosity as the soil is locally compacted (Nikolinakou et al., 2014). The static model does not simulate the radial diapir expansion, and stresses change only as a result of stress relaxation. Hence, the stress path in the static model is similar to that of Point A, showing increase mainly in the shear stress and little change in the mean stress.

The two models predict similar results for the final stress state and final porosity for a soil element near the upper part of the diapir (Fig. 8). On the basis of these current-day stress conditions, it appears that the two methodologies would give the same densities, P-wave velocities, and shear characteristics. Hence, static analysis could be an efficient and cost-effective approach for many practical applications. However, the two simulations describe very different stress histories (Fig. 8). Specifically, the evolutionary model predicts change in volume caused by horizontal shortening due to the thrust loading. In other words, the two loading histories densify the material in dissimilar ways, which could affect the microstructure of the material and hence its present-day strength and deformation characteristics (Muir Wood, 1990).

4. Comparison of strains between evolutionary and static analyses

The importance of stress history for the present stress state and strength of sediments can be illustrated by identifying how strains

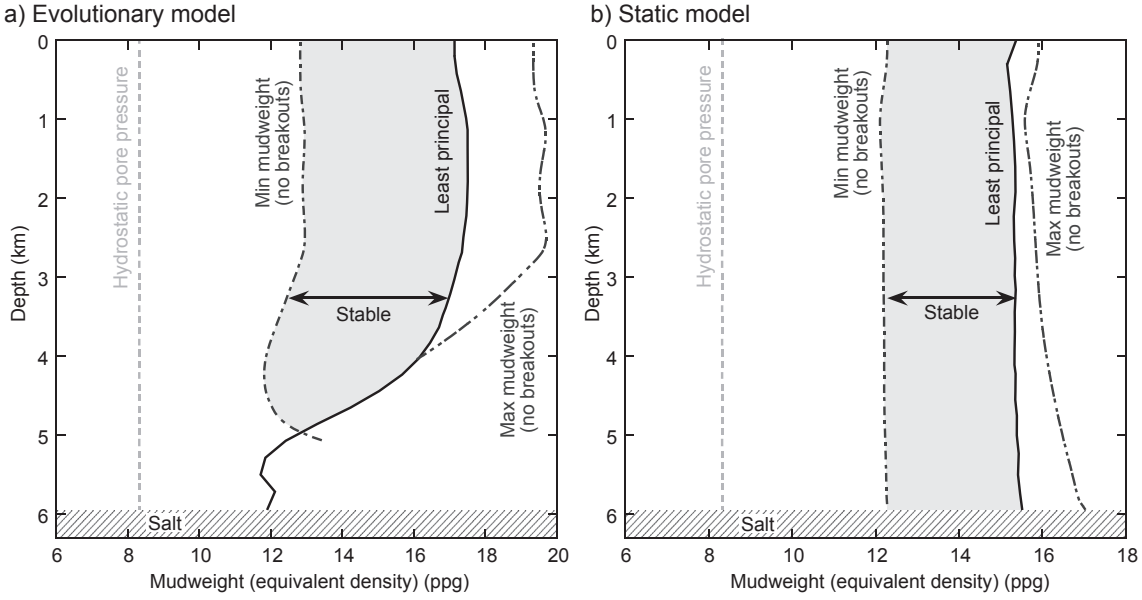

Figure 7. Mudweights predicted along well A (Fig. 5) based on a) evolutionary analysis and b) static analysis. Light gray, dashed line plots the hydrostatic pressure, which is the pore pressure in model simulations. Gray dotted and double dotted lines plot minimum and maximum mudweights that will prevent shear failure along borehole wall (breakouts). Solid black line plots least principal stress; range of stable mudweights is highlighted in light gray. Evolutionary model predicts sudden decrease in least principal stress and borehole collapse above salt base. Static model, in contrast, shows no notable change in the range of stable mudweights.

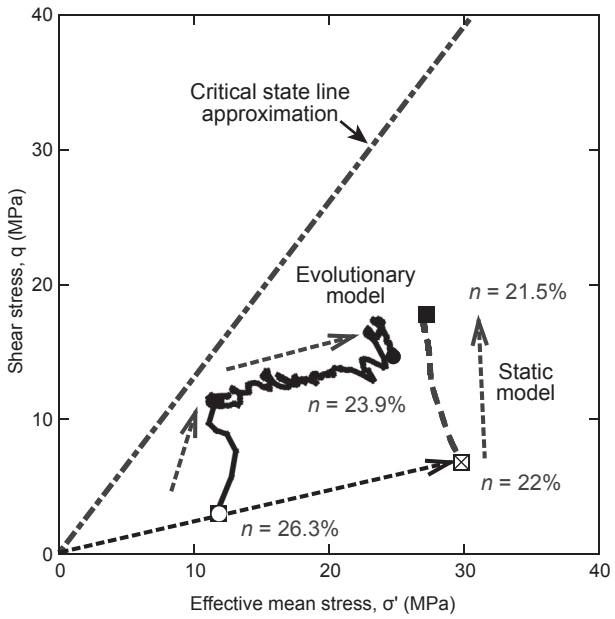

Figure 8. Stress paths during evolutionary and static analyses for Point B, near upper parts of diapir (Fig. 5). Final stress states are very similar, but analyses predict very different stress paths.

develop during the course of either simulation. The evolutionary analysis, as expected, produces significantly higher strains near the salt than does the static analysis, because the evolutionary analysis models the development of the salt cross section and the sedimentation process (Fig. 9); the final horizontal strain in the evolutionary analysis is an order of magnitude higher. The most important difference between the two approaches, though, lies in their differing predictions of shearing modes.

In order to illustrate this difference, Figure 10 shows how a soil element next to the salt diapir would be predicted to deform according to the evolutionary and static approaches (Fig. 9; elements C and D, respectively). Consider element C. Initially located at a depth of 1212 m, it is initialized with a vertical shortening of 18% owing to the uniaxial compression (burial). During the simulation of the diapir rise, the evolutionary analysis predicts an additional 4.2% of vertical shortening because of sedimentation, 8.5% horizontal shortening because of the horizontal push from the diapir, and 9.4% expansion in the hoop (circumferential) direction because of the expansion of the diapir. The major characteristic in the evolutionary analysis is the presence of large and opposing strains in the horizontal plane. In the static analysis, element D undergoes a vertical shortening of 24% during deposition; this shortening is larger than that undergone by element C because the static model is initialized at a later stage (after 2 million years of sedimentation in the evolutionary model), and hence is initially buried at the greater depth of 2450 m. During the stage of salt stress relaxation, the overall predicted strains are an order of magnitude lower than those predicted by the evolutionary analysis. Therefore, most of the volume change for element D happens during the initial uniaxial compression. The final volumes are similar (Fig. 8), however, the static element compresses to that final volume predominantly by uniaxial vertical shortening, whereas the evolutionary element undergoes large differential strains in the horizontal plane (shortening vs. extension); in other words, it undergoes significant shearing.

5. Summary and discussion

Evolutionary numerical models of rising salt diapirs describe stress redistribution in the wall rocks. Our models show a notable decrease in the hoop stress, a high increase in the radial stress and significant differential strains on horizontal cross sections.

For the sediments adjacent to a salt diapir, we compare the stress and strain patterns predicted by an evolutionary approach to those predicted by a static finite-element approach. We show that modeling the emplacement of the salt leads to very different estimates of stresses and deformations: near the base of the diapir, the evolutionary model predicts much higher levels of shear and a final stress state closer to shear failure; in addition, it captures a larger decrease in the least principal stress. Near the upper parts of the diapir, only the evolutionary model captures the radial loading of the wall rocks by the expanding salt; in addition, even though both approaches predict the same final porosity, the evolutionary model shows an increase in the mean effective stress, and differential (shear) deformations in the horizontal plane.

This work represents a first attempt to compare the differences between a static and an evolutionary approach. A complete study should also consider the coupled development of pore pressures by comparing undrained and transient results. Furthermore, slip between the salt and its wall rocks should be modeled, as it also affects the comparison between the two approaches. Nonetheless, our results demonstrate some of the limitations of static models, and the importance of capturing stress history effects.

Elevated deviatoric stresses and large shear strains are frequently observed near salt diapirs (Alsop et al., 2000; Bachrach et al., 2007; Bradley, 1978; Fredrich et al., 2003; Sweatman et al., 1999; Willson et al., 2003)). The affected wall rocks are known as drag, rubble, or brecciated zones, and they are characterized by low rock strength (Furlow, 1998). Hence, they are frequently associated with borehole collapses (e.g., Eugene Island (Bradley, 1978)). These observations highlight the importance of predicting shear stresses

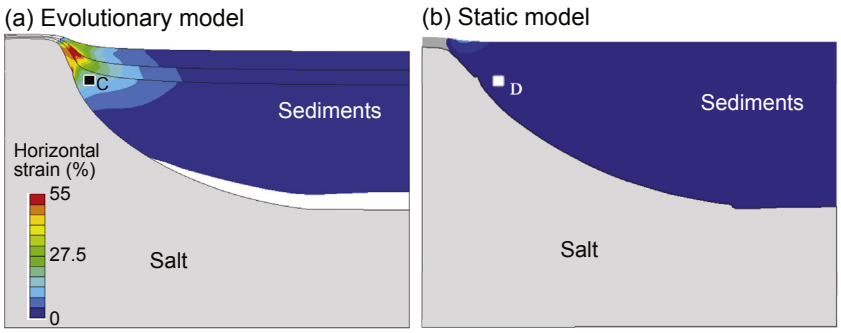

Figure 9. Horizontal strains developing during (a) evolutionary analysis; and (b) static analysis.

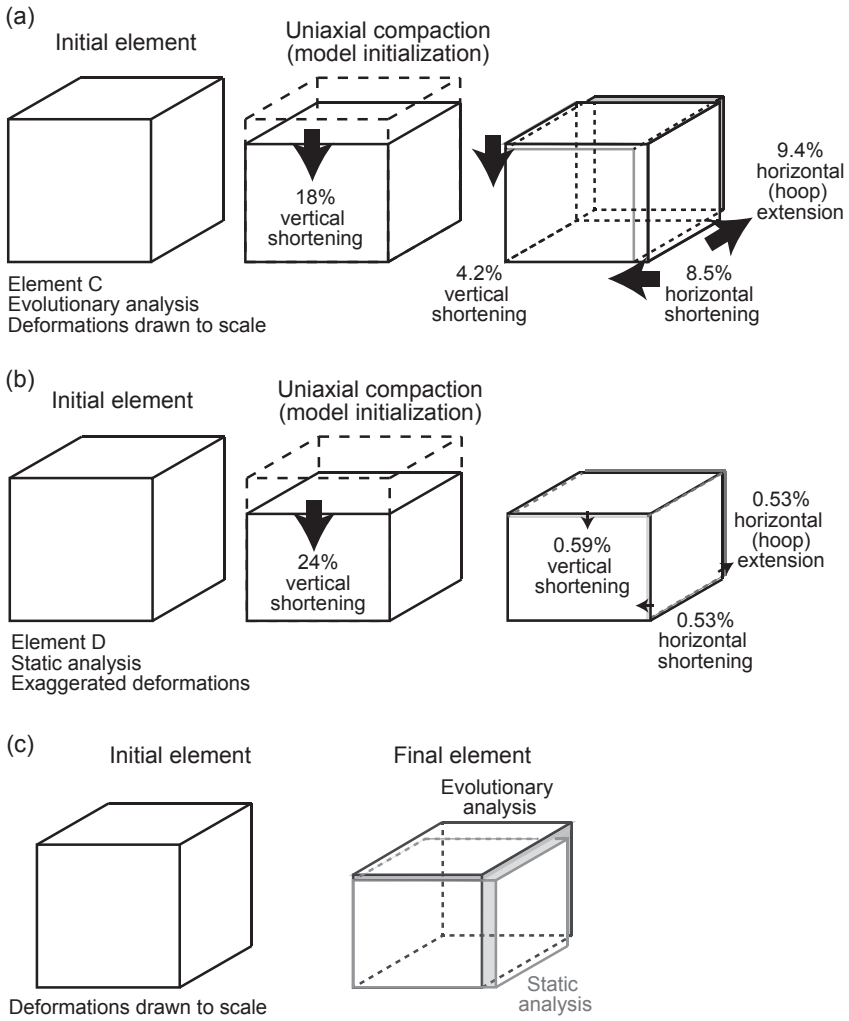

Figure 10. Deformation of soil element during evolutionary analysis (Point C in Fig. 9) and static analysis (Point D in Fig. 9). Element at C (first line of Fig. 10) is initialized at depth of about 1200 m, which corresponds to 18% vertical shortening as a result of uniaxial compression. Element D (second line of Fig. 10) initialized at greater depth, because additional 1600 m of sediments have meanwhile been deposited (Fig. 2); hence Element D has undergone larger initial vertical shortening (24%). Evolutionary model (C) predicts additional 4.2% of vertical shortening, 8.5% radial shortening, and 9.4% hoop expansion. Static model (D) predicts strains one order of magnitude lower. As a result, when comparing final elements (third line of Fig. 10), static model (light gray cube) shows mostly vertical shortening, whereas evolutionary one (dark gray) predicts differential strains on horizontal plane.

around salt. Static models can only capture the shear stresses that are related to the salt relaxation mechanism. In contrast, we showed that the evolutionary approach predicts much higher differential stresses near a salt diapir, and stress states that are close to shear failure. In addition, the evolutionary model is able to capture significant shear strains in the horizontal plane, reflecting the simultaneous increase in radial stress and decrease in hoop stress often observed (Dusseault et al., 2004; Fredrich et al., 2003; Seymour et al., 1993).

Because it does not model the circumferential expansion of the salt diapir, the static approach underestimates the decrease in hoop stress. However, low hoop-stress values are often reported near salt diapirs and are often associated with borehole instability and loss of circulation. Bradley (1978) attributed borehole instabilities near a salt diapir at Eugene Island to significantly lowered hoop stress near the flank of the diapir. Dusseault et al. (2004) discussed an exceptionally low minimum principal stress value above a Gulf of Guinea salt diapir; this resulted in massive loss of circulation and 92 days of lost drilling time. Seymour et al. (1993) also attributed borehole instabilities near a salt diapir to a significantly lowered hoop stress near the flanks, and note that these problems led to a nonproductive drilling time of 26.3%. In contrast to the static approach, the evolutionary approach is able to predict a decrease in hoop stress near the salt diapir. Therefore, the evolutionary approach is able to capture the sudden decrease in the least principal stress near the base salt, as well as foresee a high probability of borehole breakouts (Fig. 7).

Finally, several authors have reported elevated radial stresses near the upper parts of a salt diapir (Bradley, 1978; Dusseault et al., 2004). The static approach can only model deformations caused by salt relaxation; hence it can predict elevated lateral stresses only when the salt geometry is predominantly horizontal (Nikolinakou et al., 2013). In contrary, the evolutionary approach captures the significant radial strains associated with the rising of the diapir (Fig. 9), and therefore is able to predict radial stresses that are comparable or even higher than the overburden value (Nikolinakou et al., 2014).

Overall, these published observations of stresses and shear failures around salt diapirs highlight the importance of modeling the radial and circumferential expansion associated with the rise of

a salt diapir. Furthermore, the evolutionary approach can provide a detailed description of the stress history of the wall-rock sediments, which is essential for understanding how the material has compressed to its current volume, and therefore for predicting more efficiently the current strength and anisotropy characteristics of the wall rocks.

Acknowledgments

The project was funded by the Applied Geodynamics Laboratory consortium (AGL) and the GeoFluids consortium at The University of Texas at Austin (UT GeoFluids). AGL is supported by the following companies: Anadarko, Apache, BHP Billiton, BP, CGGVeritas, Chevron, Cobalt, Conoco-Phillips, Ecopetrol, ENI, ExxonMobil, Fugro, Global Geophysical Services, Hess, IMP, Ion, Korea National Oil, McMoRan, Maersk, Marathon, Murphy, Nexen, Noble, Pemex, Petrobras, PGS, Repsol, Samson, Saudi Aramco, Shell, Statoil, TGS, Total, WesternGeco, and Woodside. UT GeoFluids is supported by the following companies: Anadarko, BHP Billiton, BP, Chevron, Conoco-Phillips, ExxonMobil, Hess, Schlumberger, Shell, Statoil and Total. The authors received additional support from the Jackson School of Geosciences at The University of Texas. The text was edited by Chris Parker. Publication authorized by the Director, Bureau of Economic Geology.

Appendix A. Material input

Table A1
Input material parameter values for the Munson–Dawson model for salt in Elfen (Fredrich et al., 2007; Munson, 1997; Munson and Dawson, 1979).

Parameter	Units	Value
E	MPa	10,000
V	–	0.35
P	kg/m^3	2200
A_1	1/s	1.885E + 36
N_1	–	5.5
Q_1	cal/mol	25,000
A_2	1/s	2.17E + 26
N_2	cal/mol	5.0
Q_2	–	10,000
R	cal/°C/mol	1.987
T_0	°C	10
T_{CONST}	°C	273
G_0	MPa	12,400
dG/dT	GPa/°K	10.0

Table A2
Input material parameter values for the SR3 model for the sediments in Elfen (Nygard et al., 2006, 2004; Rockfield, 2010).

Parameter	Units	Value
E	MPa	40
ν	–	0.25
ρ	kg/m^3	Figure 1
K_0	MPa	10
K	–	0.01
$p_{t,0}$	MPa	0.085
$p_{c,0}$	MPa	−1.00
β	°	60°
ψ	°	51°
β_0	–	0.60
β_1	1/MPa	0.725
α	–	0.25
N	–	1.3
n_0	–	0.38
Hardening properties		Figure A1

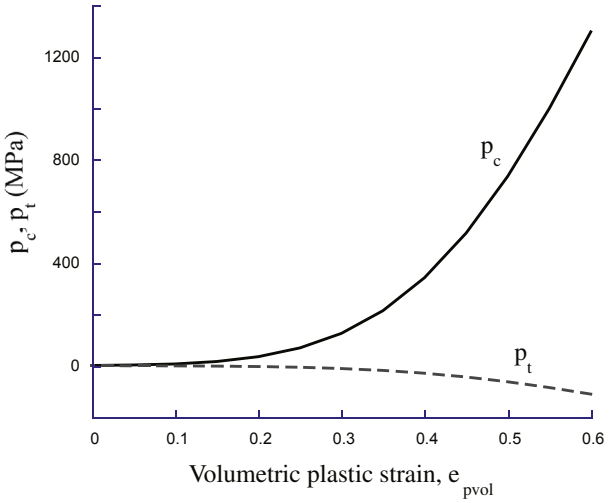

Figure A1. Input hardening properties for SR3 (Rockfield, 2010).

Table A3
Input parameters for the viscoelastic salt model in Abaqus.

Parameter	Description	Units	Value
P	Density	kg/m^3	2200
E	Young's modulus	GPa	10
V'	Poisson's ratio	–	0.35
η	Viscosity	kPa s	10^{15}

Table A4
Input parameters for the Modified Cam Clay sediment model in Abaqus.

Parameter	Description	Units	Value
ρ	Density	kg/m^3	2230
λ	Elastoplastic slope of e-lnσ' plot	–	0.085
κ	Elastic slope of e-lnσ' plot	–	0.012
ϕ'_{TC}	Friction angle in Triaxial Compression	°	30°
ν'	Poisson's ratio	–	0.225
e_0	Initial void ratio (at the depth of the salt)	–	0.5
K_0	Coefficient of earth pressure at rest	–	0.8

References

Abaqus User Guide and Help Documentation. SIMULIA Company.

Adachi, J., Nagy, Z.R., Sayers, C.M., Smith, M., Becker, D.F., 2012. Drilling adjacent to salt bodies: definition of mud weight window and pore pressure using numerical models and fast well planning tool. In: SPE Annual Technical Conference and Exhibition, 8–10 October 2012, San Antonio, Texas, USA, 10.2118/159739-ms.

Albertz, M., Beaumont, C., 2010. An investigation of salt tectonic structural styles in the Scotian Basin, offshore Atlantic Canada: 2. Comparison of observations with geometrically complex numerical models. Tectonics 29, TC4018. http://dx.doi.org/10.1029/2009tc002540.

Albertz, M., Beaumont, C., Shimeld, J.W., Ings, S.J., Gradmann, S., 2010. An investigation of salt tectonic structural styles in the Scotian Basin, offshore Atlantic Canada: 1. Comparison of observations with geometrically simple numerical models. Tectonics 29, TC4017. http://dx.doi.org/10.1029/2009tc002539.

Allen, J., Beaumont, C., 2012. Impact of inconsistent density scaling on physical analogue models of continental margin scale salt tectonics. J. Geophys. Res. Solid Earth 117, B08103. http://dx.doi.org/10.1029/2012jb009227.

Alsop, G.I., Brown, J.P., Davison, I., Gibling, M.R., 2000. The geometry of drag zones adjacent to salt diapirs. J. Geol. Soc. 157, 1019–1029. http://dx.doi.org/10.1144/jgs.157.5.1019.

Bachrach, R., Sengupta, M., Salama, A., 2007. Stress and seismic anisotropy near salt bodies – numerical modeling and observation from wide-azimuth marine data. In: EAGE 69th Conference & Exhibition, 11–14 June 2007, London, UK.

Beltrão, R.L.C., Sombra, C.L., Lage, A.C.V.M., Fagundes Netto, J.R., Henriques, C.C.D., 2009. Challenges and new technologies for the development of the pre-salt cluster, Santos Basin, Brazil. In: Offshore Technology Conference, 4–7 May 2009, at Houston, Texas, 10.4043/19880-MS.

Bradley, W.B., 1978. Borehole failure near salt domes. In: Society of Petroleum Engineers Annual Fall Technical Conference and Exhibition, 10/01/1978, Houston, Texas.

Chemia, Z., Schmeling, H., Koyi, H., 2009. The effect of the salt viscosity on future evolution of the Gorleben salt diapir, Germany. Tectonophysics 473, 446–456. http://dx.doi.org/10.1016/j.tecto.2009.03.027.

Crook, A.J.L., Willson, S.M., Yu, J.G., Owen, D.R.J., 2006. Predictive modelling of structure evolution in sandbox experiments. J. Struct. Geol. 28, 729–744. http://dx.doi.org/10.1016/j.jsg.2006.02.002.

Dusseault, M.B., Maury, V., Sanfilippo, F., Santarelli, F.J., 2004. Drilling around salt: risks, stresses, and uncertainties. In: US Rock Mechanics and Geomechanics Symposium, 5–9 June 2004 paper 04–647.

Fredrich, J.T., Coblentz, D., Fossum, A.F., Thorne, B.J., 2003. Stress perturbations adjacent to salt bodies in the deepwater Gulf of Mexico. In: Society of Petroleum Engineers Annual Technical Conference and Exhibition, 5–8 October 2003, Denver, Colorado.

Fredrich, J.T., Fossum, A.F., Hickman, R.J., 2007. Mineralogy of deepwater Gulf of Mexico salt formations and implications for constitutive behavior. J. Pet. Sci. Eng. 57, 354–374. http://dx.doi.org/10.1016/j.petrol.2006.11.006.

Furlow, W., Dec 1998. Anadarko uses subsalt know-how to beat the odds. Offshore, 96–98.

Goteti, R., Ings, S.J., Beaumont, C., 2012. Development of salt minibasins initiated by sedimentary topographic relief. Earth Planet. Sci. Lett. 339/340, 103–116. http://dx.doi.org/10.1016/j.epsl.2012.04.045.

Gradmann, S., Beaumont, C., Albertz, M., 2009. Factors controlling the evolution of the Perdido Fold Belt, northwestern Gulf of Mexico, determined from numerical models. Tectonics 28, TC2002. http://dx.doi.org/10.1029/2008tc002326.

Henk, A., 2005. Pre-drilling prediction of the tectonic stress field with geomechanical models. First Break 23, 53–57. http://dx.doi.org/10.3997/1365-2397.2005021.

Koupriantchik, D., Hunt, S.P., Boult, P.J., Meyers, A.G., 2005. Geomechanical modeling of salt diapirs: 3D salt structure from the officer Basin, South Australia. In: Central Australian Basins Symposium.

Koupriantchik, D., Meyers, A.G., Hunt, S., 2004. 3D geomechanical modelling towards understanding stress anomalies causing wellbore instability. In: Gulf Rocks 2004, the 6th North America Rock Mechanics Symposium (NARMS), June 5–9, 2004, Houston, Texas.

Lewis, R.W., Schrefler, B.A., 1987. The Finite Element Method in the Deformation and Consolidation of Porous Media Chichester [Sussex]. Wiley, New York.

Luo, G., Nikolinakou, M.A., Flemings, P.B., Hudec, M.R., 2012a. Geomechanical modeling of stresses adjacent to salt bodies: 1. Uncoupled models. AAPG Bull. 96, 43–64. http://dx.doi.org/10.1306/04111110144.

Luo, G., Nikolinakou, M.A., Flemings, P.B., Hudec, M.R., 2012b. Near-salt stress and wellbore stability: a finite-element study and its application. In: 46th US Rock Mechanics and Geomechanics Symposium, Chicago, IL paper 12–309.

Mackay, F., Inoue, N., Fontoura, S.A.B., Botelho, F., 2008. Geomechanical effects of a 3D vertical salt well drilling by FEA. In: 42nd U.S. Rock Mechanics Symposium (USRMS), June 29–July 2, 2008, San Francisco, California paper 08–041.

Matthews, W.R., Kelly, J., 1967. How to predict formation pressure and fracture gradient. Oil Gas J. 20, 92–106.

Meyer, D., Zarra, D., Rains, D., Meltz, B., Hall, T., May 2005. Emergence of the Lower Tertiary Wilcox trend in the deepwater Gulf of Mexico. World Oil, 72–77.

Muir Wood, D., 1990. Soil Behaviour and Critical State Soil Mechanics. Cambridge University Press, Cambridge, U.K.

Munson, D.E., 1997. Constitutive model of creep in rock salt applied to underground room closure. Int. J. Rock Mech. Min. Sci. 34, 233–247. http://dx.doi.org/10.1016/S0148-9062(96)00047-2.

Munson, D.E., Dawson, P.R., 1979. Constitutive Model for the Low Temperature Creep of Salt (with Application to WIPP). SAND79-1853. Sandia National Laboratories, Albuquerque, NM.

Nikolinakou, M.A., Flemings, P.B., Hudec, M.R., 2014. Modeling stress evolution around a rising salt diapir. Mar. Pet. Geol. 51, 230–238. http://dx.doi.org/10.1016/j.marpetgeo.2013.11.021.

Nikolinakou, M.A., Luo, G., Hudec, M.R., Flemings, P.B., 2012. Geomechanical modeling of stresses adjacent to salt bodies: 2. poro-elasto-plasticity and coupled overpressures. Am. Assoc. Pet. Geol. Bull. 96, 65–85. http://dx.doi.org/10.1306/04111110143.

Nikolinakou, M.A., Merrell, M.P., Luo, G., Flemings, P.B., Hudec, M.R., 2013. Geomechanical modeling of the Mad Dog salt, Gulf of Mexico. In: 47th US Rock Mechanics Symposium, San Francisco, CA, 23–26 June, 2013 paper 13–234.

Nygard, R., Gutierrez, M., Bratli, R.K., Hoeg, K., 2006. Brittle-ductile transition, shear failure and leakage in shales and mudrocks. Mar. Pet. Geol. 23, 201–212. http://dx.doi.org/10.1016/j.marpetgeo.2005.10.001.

Nygard, R., Gutierrez, M., Gautam, R., Hoeg, K., 2004. Compaction behavior of argillaceous sediments as function of diagenesis. Mar. Pet. Geol. 21, 349–362. http://dx.doi.org/10.1016/j.marpetgeo.2004.01.002.

Orlic, B., Wassing, B.B.T., 2013. A study of stress change and fault slip in producing gas reservoirs overlain by elastic and viscoelastic caprocks. Rock Mech. Rock Eng. 46, 421–435. http://dx.doi.org/10.1007/s00603-012-0347-6.

Peric, D., Crook, A.J.L., 2004. Computational strategies for predictive geology with reference to salt tectonics. Comput. Methods Appl. Mech. Eng. 193, 5195–5222. http://dx.doi.org/10.1016/j.cma.2004.01.037. ELFEN Forward Modeling User Manual.

Rockfield, 2010. ELFEN Forward Modeling User Manual..

Rowan, M.G., Ratliff, R.A., 2012. Cross-section restoration of salt-related deformation: best practices and potential pitfalls. J. Struct. Geol. 41, 24–37. http://dx.doi.org/10.1016/j.jsg.2011.12.012.

Sanz, P., Gray, G., Albertz, M., 2011. Finite element modeling of in-situ stresses near salt bodies. In: Abstract T51C-2353, Presented at 2011 Fall Meeting, AGU, San Francisco, Calif., 5–9 Dec.

Sanz, P.F., Dasari, G.R., 2010. Controls on in-situ stresses around salt bodies. In: 44th Rock Mechanics and Geomechanics Symposium, Salt Lake City, UT June 27–30 paper 10–169.

Schultz-Ela, D.D., 2003. Origin of drag folds bordering salt diapirs. AAPG Bull. 87, 757–780.

Schutjens, P.M., Snippe, J.R., Mahani, H., Turner, J., Ita, J., Mossop, A.P., 2010. Production-induced stress change in and above a reservoir pierced by two salt domes: geomechanical modeling and its applications. In: SPE EUROPEC/EAGE Annual Conference and Exhibition, 14–17 June, Barcelona, Spain, 10.2118/131590-MS.

Seymour, K.P., Rae, G., Peden, J.M., Ormston, K., 1993. Drilling close to salt diapirs in the North Sea. In: Offshore Europe, 09/07/1993, Aberdeen, U.K.

Sweatman, R., Faul, R., Ballew, C., 1999. New solutions for subsalt-well lost circulation and optimized primary cementing. In: SPE Annual Technical Conference and Exhibition, 10/03/1999, Houston, Texas.

Terzaghi, K., Peck, R.B., Mesri, G., 1996. Soil Mechanics in Engineering Practice. Wiley, New York.

Thornton, D.A., Roberts, D.T., Crook, A.J.L., Yu, J.G., 2011. Regional scale salt tectonics modelling: bench-scale validation and extension to field-scale problems. In: Beyond Balanced Sections: Geological Society of America Conference, at Minneapolis, USA.

Urai, J.L., Spiers, C.J., 2007. The effect of grain boundary water on deformation mechanisms and rheology of rocksalt during long-term deformation. In: 6th Conference on the Mechanical Behavior of Salt, 'SaltMech6', 22–25 May 2007, at Hannover, Germany.

Willson, S.M., Edwards, S., Heppard, P.D., Li, X., Coltrin, G., Chester, D.K., Harrison, H.L., Cocales, B.W., 2003. Wellbore stability challenges in the deep water, Gulf of Mexico: case history examples from the Pompano field. In: SPE Annual Technical Conference and Exhibition, 5–8 October 2003, Denver, Colorado.

Zhang, J., William, S., Chris, L., 2008. Casing ultradeep, ultralong salt sections in deep water: a case study for failure diagnosis and risk mitigation in record-depth well. In: Society of Petroleum Engineers Annual Technical Conference and Exhibition, 09/21/2008, Denver, Colorado, USA.

Zoback, M.D., 2007. Reservoir Geomechanics, first ed. Cambridge University Press.

Zoback, M.D., Healy, J.H., 1984. Friction, faulting and in situ stress. Ann. Geophys. 2, 689–698.